

This discussion paper is/has been under review for the journal *Atmospheric Chemistry and Physics (ACP)*. Please refer to the corresponding final paper in *ACP* if available.

**Smoke plume rise in  
a windy environment**

S. R. Freitas et al.

# Technical Note: Sensitivity of 1-D smoke plume rise models to the inclusion of environmental wind drag

S. R. Freitas<sup>1</sup>, K. M. Longo<sup>2</sup>, J. Trentmann<sup>3,\*</sup>, and D. Latham<sup>4</sup>

<sup>1</sup>Center for Weather Forecasting and Climate Studies, INPE, Cachoeira Paulista, Brazil

<sup>2</sup>Center for Space and Atmospheric Sciences, INPE, São José dos Campos, Brazil

<sup>3</sup>University of Mainz, Mainz, Germany

<sup>4</sup>USDA Forest Service, Montana, USA

\* now at: German Weather Service, Offenbach, Germany

Received: 29 May 2009 – Accepted: 29 June 2009 – Published: 7 July 2009

Correspondence to: S. R. Freitas (saulo.freitas@cptec.inpe.br)

Published by Copernicus Publications on behalf of the European Geosciences Union.

Title Page

Abstract

Introduction

Conclusions

References

Tables

Figures

◀

▶

◀

▶

Back

Close

Full Screen / Esc

Printer-friendly Version

Interactive Discussion



## Abstract

We revisit the parameterization of the vertical transport of hot gases and particles emitted from biomass burning, described in Freitas et al. (2007), to include the effects of environmental wind on transport and dilution of the smoke plume at the cloud scale.

5 Typically, the final vertical height that the smoke plumes reach is controlled by the thermodynamic stability of the atmospheric environment and the surface heat flux released by the fire. However, the presence of a strong horizontal wind can enhance the lateral entrainment and induce additional drag, particularly for small fires, impacting the smoke injection height. This process is quantitatively represented by introducing  
10 an additional entrainment term to account for organized inflow of a mass of cooler and drier ambient air into the plume and its drag by momentum transfer. An extended set of equations including the horizontal motion of the plume and the additional increase of the plume radius is solved to explicitly simulate the time evolution of the plume rise with the additional mass and momentum. One-dimensional (1-D) model results are  
15 presented for two deforestation fires in the Amazon basin with sizes of 10 and 50 ha under calm and windy atmospheric environments. The results are compared to corresponding simulations generated by the complex non-hydrostatic three dimensional (3-D) Active Tracer High resolution Atmospheric Model (ATHAM). We show that the 1-D  
20 model results compare well with the full 3-D simulations. The 1-D model may thus be used in field situations where extensive computing facilities are not available, especially under conditions for which several optional cases must be studied.

## 1 Introduction

Biomass burning emits hot gases and particles which are transported upward by the positive buoyancy generated by the fire. Due to radiative cooling and the efficient heat  
25 transport by convection, there is a rapid decay of temperature above the burning area. Also, the interaction between the smoke and the environment produces eddies that

## Smoke plume rise in a windy environment

S. R. Freitas et al.

Title Page

Abstract

Introduction

Conclusions

References

Tables

Figures

◀

▶

◀

▶

Back

Close

Full Screen / Esc

Printer-friendly Version

Interactive Discussion



**Smoke plume rise in a windy environment**

S. R. Freitas et al.

[Title Page](#)[Abstract](#)[Introduction](#)[Conclusions](#)[References](#)[Tables](#)[Figures](#)[I◀](#)[▶I](#)[◀](#)[▶](#)[Back](#)[Close](#)[Full Screen / Esc](#)[Printer-friendly Version](#)[Interactive Discussion](#)

entrain colder environmental air into the smoke plume, which dilutes the plume and reduces buoyancy. The dominant characteristic is a strong upward flow with a moderate temperature excess from the ambient. The final height that the plume reaches is controlled by the thermodynamic stability of the atmospheric environment and the surface heat flux release from the fire. Moreover, additional buoyancy may be gained from latent heat release of condensation and plays an important role in determining the effective injection height of the plume, that is, its terminal height. However, the occurrence of strong horizontal wind can enhance lateral entrainment and can even prevent the plume's reaching the condensation level, particularly for small fires, severely impacting the injection height. This effect is shown by two photographs of the smoke plume rise produced from two different deforestation fires in the Amazon basin (Fig. 1). The plume shown on the left moves upward with only a slight deviation from the vertical, indicating plume development in a calm environment. However, the plume on the right shows much stronger deflection from the vertical, an indication of a windy environment. Note that both plumes are capped by cumulus, indicating that cloud microphysics might have had a significant role in the plume development.

The effect of ambient wind on the plume rise from volcanic sources has been studied by several authors. Graf et al. (1999) performed a set of sensitivity studies using a two-dimensional version of the Active Tracer High resolution Atmospheric Model (described here in Sect. 3.2) as a non-hydrostatic volcano plume model with explicit treatment of turbulence and microphysics. The authors applied this modeling system to simulate the impacts of environmental conditions on the vertical plume development. They found that, in general, a horizontal wind reduces the height reached by the plume. All environmental impacts were found to strongly depend on the intensity of the entrainment and, thus, on the quality of the calculated turbulence properties. Bursik (2001) applied a 1-D theoretical model of a plume to study the interaction between a volcanic plume and an ambient wind. He also shows that the enhanced entrainment from the wind decreases the plume rise height, mainly at altitudes with the high wind speeds of the polar jet.

**Smoke plume rise in a windy environment**

S. R. Freitas et al.

[Title Page](#)[Abstract](#)[Introduction](#)[Conclusions](#)[References](#)[Tables](#)[Figures](#)[I◀](#)[▶I](#)[◀](#)[▶](#)[Back](#)[Close](#)[Full Screen / Esc](#)[Printer-friendly Version](#)[Interactive Discussion](#)

In this technical note we revisit a 1-D parameterization of the vertical transport of hot gases and particles emitted from vegetation fires, described in Freitas et al. (2007, hereafter F2007), to include the effects of environmental wind on transport and dilution of the smoke plume at the cloud scale. This process is quantitatively represented by introducing an additional entrainment term to represent the organized inflow of the ambient air into the plume, as well as the drag on the plume by the external ambient wind. The extra entrainment enhances the in-cloud mixing with the cooler and drier ambient air. The net effect on the dynamics is a reduction of the in-cloud velocity in the vertical through momentum transfer to the entrained air mass; while horizontally, there is a strong acceleration in the nearby surface layer as well as in the layers with strong ambient wind shear. An extended set of equations, including the horizontal motion of the plume and the additional increase of the plume size, is now solved to explicitly simulate the time evolution of the plume rise and determine the final injection layer. This information is then used to determine the vertical layers of 3-D low resolution atmospheric chemistry-transport models, in which trace gases and aerosols emitted during the flaming phase of the vegetation fires are released, transported and dispersed.

This technical note is organized as follows. In Sect. 2, the methodology is described. Section 3, Part 1 discusses the dynamics and thermodynamics of the case studies. In parts 2 and 3, numerical simulations with 3-D ATHAM and the 1-D plume models are introduced and compared. Conclusions are discussed in Sect. 4.

## 2 Methodology

The smoke plume rise associated to the biomass burning is explicitly simulated using a simple one-dimensional time-dependent entrainment plume model (Latham, 1994, F2007; hereafter 1-D PRM). Equations (1) to (7) introduce this 1-D PRM, modified to include the horizontal ambient wind effect (here our discussion emphasizes the new terms where the quantity appears and the Eqs. (6) and (7), a detailed description of

the original set of equations can be found in F2007):

$$\frac{\partial w}{\partial t} + w \frac{\partial w}{\partial z} = \frac{1}{1 + \gamma} g B - \frac{2\alpha}{R} w^2 - \delta_{\text{entr}} w \quad (1)$$

$$\frac{\partial T}{\partial t} + w \frac{\partial T}{\partial z} = -w \frac{g}{c_p} - \frac{2\alpha}{R} |w| (T - T_e) - \delta_{\text{entr}} (T - T_e) + \left( \frac{\partial T}{\partial t} \right)_{\text{micro-physics}} \quad (2)$$

$$\frac{\partial r_v}{\partial t} + w \frac{\partial r_v}{\partial z} = -\frac{2\alpha}{R} |w| (r_v - r_{v_e}) - \delta_{\text{entr}} (r_v - r_{v_e}) + \left( \frac{\partial r_v}{\partial t} \right)_{\text{micro-physics}} \quad (3)$$

$$5 \quad \frac{\partial r_c}{\partial t} + w \frac{\partial r_c}{\partial z} = -\frac{2\alpha}{R} |w| r_c - \delta_{\text{entr}} r_c + \left( \frac{\partial r_c}{\partial t} \right)_{\text{micro-physics}} \quad (4)$$

$$\frac{\partial r_{\text{ice,rain}}}{\partial t} + w \frac{\partial r_{\text{ice,rain}}}{\partial z} = -\frac{2\alpha}{R} |w| r_{\text{ice,rain}} - \delta_{\text{entr}} r_{\text{ice,rain}} + \left( \frac{\partial r_{\text{ice,rain}}}{\partial t} \right)_{\text{micro-physics}} + \text{sedim}_{\text{ice,rain}} \quad (5)$$

$$\frac{\partial u}{\partial t} + w \frac{\partial u}{\partial z} = -\frac{2\alpha}{R} |w| (u - u_e) - \delta_{\text{entr}} (u - u_e) \quad (6)$$

$$\frac{\partial R}{\partial t} + w \frac{\partial R}{\partial z} = +\frac{6\alpha}{5R} |w| R + \frac{1}{2} \delta_{\text{entr}} R \quad (7)$$

Here  $w$ ,  $T$ ,  $r_v$ ,  $r_c$ ,  $r_{\text{rain}}$ ,  $r_{\text{ice}}$  are the vertical velocity, air temperature, water vapor, cloud, rain and ice mixing ratios, respectively, and are associated with in-cloud air parcels. The velocity  $u$  represents the horizontal velocity of the center of mass of the

Title Page

Abstract

Introduction

Conclusions

References

Tables

Figures

◀

▶

◀

▶

Back

Close

Full Screen / Esc

Printer-friendly Version

Interactive Discussion



## Smoke plume rise in a windy environment

S. R. Freitas et al.

plume at level  $z$ . In the equations above the index  $e$  stands for the environmental value. The traditional entrainment coefficient is given by  $2\alpha R^{-1}$ , where  $R$  is the radius of the plume and  $\alpha=0.05$ . In an ambient wind, the relative horizontal motion between the plume and the ambient air enhances the lateral entrainment through a “collisional” process promoting an additional exchange of momentum, energy, water, trace gases and aerosols between both air masses. We assume instantaneous mixing between in-cloud and ambient properties inside the plume. To quantitatively include this process, we add an extra entrainment term called “dynamic entrainment” ( $\delta_{\text{entr}}$ ) formulated as

$$\delta_{\text{entr}} = \frac{2}{\pi R} (u_e - u) \quad (8)$$

where all variables are as previously defined. The dynamic entrainment term is proportional to the difference between the magnitudes of the ambient and plume air horizontal velocities, because there is no dynamic entrainment when both masses are moving at the same speed. Also,  $\delta_{\text{entr}}$  is inversely proportional to the plume radius size meaning that the bigger the plume, the less sensitive it is to this entrainment process. The derivation of Eq. (8) is given in Appendix A.

Equation (1) is the vertical equation of motion. The new term ( $-\delta_{\text{entr}} w$ ) expresses the loss rate of in-cloud vertical velocity due to momentum transfer to the ambient air mass entrained into the plume (environmental vertical velocity is supposed negligible when compared to the in-cloud vertical velocity). Equations (2–5) express the first law of thermodynamics and mass continuity equations for water phases including the dynamic entrainment process. This process is included using the traditional bulk formulation, being expressed by the product of the entrainment rate and the difference between in-cloud and ambient values.

Equation (6) is introduced to represent the gain of horizontal velocity of the plume due to drag by the ambient air flow. The entrainment terms are responsible for the bent-over plumes as seen in Fig. 1. The lower boundary condition for the solution ( $u$ ) of this equation is  $u(z=0)=0$ . From Eq. (6), with no wind ( $u_e(z)=0$ ), the plume will develop only vertical motion, reducing to the original solution of F2007. Equation (7) represents

Title Page

Abstract

Introduction

Conclusions

References

Tables

Figures

◀

▶

◀

▶

Back

Close

Full Screen / Esc

Printer-friendly Version

Interactive Discussion



the increase of plume radius size due to the entrainment, in this case amplified by the organized inflow of ambient air. In ambient at rest, Eq. (7) reduces to the traditional Turner style plume (Turner, 1973; Latham, 1994). The lower boundary condition for the solution of Eq. (7) is obtained from the fire size and burning mass.

### 3 Case studies and 1-D PRM comparisons with the ATHAM model

#### 3.1 Description of the case studies

To evaluate model performance and sensitivity to the new formulation for simulating the plume rise of Amazon basin deforestation fires under different environmental conditions, we performed a set of numerical experiments using two selected thermodynamical situations. Figure 2 shows the two cases obtained from rawinsondes launched in the burning season of 2002 in the Amazon basin over a forested site and close to deforestation areas. Figure 2a depicts a typical atmospheric condition on Amazon basin and central part of South America during the burning season at 1800Z, normally the peak time of the diurnal cycle of basin fires. A rawinsonde, launched at 1800Z on 20 September 2002, shows a strong thermal inversion around 800 hPa with a very dry layer above, labeled as the dry case. On the other side of Fig. 2, the atmosphere is described by a rawinsonde launched one week later and on the same region (Fig. 2b) which is quite different. There was a weaker thermal inversion around 870 hPa and a much moister layer above compared with the dry case, was labeled as the wet case. In addition, these two cases also present a significant difference in the horizontal wind magnitude (see Fig. 2c). For the dry case, the mean magnitude is approximately  $2 \text{ m s}^{-1}$  from the surface to 500 hPa while the wet case has values of approximately 4 to  $5 \text{ m s}^{-1}$ . Note also that there is strong wind shear in the first 1500 m for both situations, from 2 to  $4 \text{ m s}^{-1}$  and 2 to  $6 \text{ m s}^{-1}$  for dry and wet cases, respectively. The comparison between the two cases is interesting due to the different roles that cloud microphysics and ambient wind processes play on the position of the smoke injection

Title Page

Abstract

Introduction

Conclusions

References

Tables

Figures

◀

▶

◀

▶

Back

Close

Full Screen / Esc

Printer-friendly Version

Interactive Discussion



layer.

## 3.2 Description and results of the ATHAM model runs

The Active Tracer High resolution Atmospheric Model (Oberhuber et al., 1998) is a three-dimensional atmospheric plume model, which has been designed and employed for the simulation of strong convective events, e.g., volcanic eruptions (e.g., Graf et al., 1999; Herzog et al., 2003; Textor et al., 2003) and vegetation fires (e.g., Trentmann et al., 2002, 2006; Luderer et al., 2006). ATHAM solves the Navier-Stokes equation for a gas-particle mixture, based on external forcing including the transport of active tracers. Cloud microphysical processes are simulated using a two-moment scheme that predicts the numbers and mass mixing ratios of four hydrometeor classes and water vapor (Textor et al., 2006).

Fire emissions are represented in ATHAM by prescribing emission fluxes into the lowest atmospheric model layer over specified fire grid boxes. In the present study, only fluxes of heat, moisture and aerosol particles are considered. The model simulations presented here were conducted on a stretched grid with a minimum horizontal and vertical model grid spacing of  $50\text{ m} \times 50\text{ m} \times 50\text{ m}$  in the center and increasing grid spacing towards the edges of the model domain. The total model domain covered  $15\text{ km} \times 15\text{ km} \times 23\text{ km}$  corresponding to  $86 \times 86 \times 80$  grid boxes. The maximum time step was set to 1.5 s, the minimum time step was determined dynamically by the Courant-Friedrich-Lewy (CFL) criterion. The heat flux and its temporal evolution were set as for the 1-D PRM model. Figure 3 presents the horizontally averaged aerosol mass distributions at different times after model start for a fire with a size of 10 ha and a heat flux of  $80\text{ kW m}^{-2}$  for the dry (panel A) and the wet cases (panel B). To convert the heat flux to convective energy, the McCarter and Broido (1965) factor (0.55) is used. The main simulated outflow height of the dry case is slightly below 4 km, while the outflow height of the wet case is at around 1.5 km. The differences in the outflow height are determined by the different atmosphere thermodynamic stabilities of the profiles (Fig. 2a and b) and the differences in the wind profiles (see Fig. 2c) with a stronger horizon-

## Smoke plume rise in a windy environment

S. R. Freitas et al.

Title Page

Abstract

Introduction

Conclusions

References

Tables

Figures

◀

▶

◀

▶

Back

Close

Full Screen / Esc

Printer-friendly Version

Interactive Discussion



tal wind in the wet case. In Fig. 3b results from four simulation times are presented demonstrating that the emission height reaches an equilibrium level after 30 min of simulation. Figure 3c and d show results from ATHAM simulations assuming a fire with a size of 50 ha. As expected, in both cases the emission height reaches higher altitudes than in the case of the 10 ha fire. The thermodynamic structures of the profiles show a narrow altitude distribution of the aerosols in the wet case near 4 km, while the aerosol is spread between 4 and 6 km in the dry case.

### 3.3 Description and results of 1-D PRM model runs

The 1-D PRM was run using a constant grid space resolution of 100 m with a top at 20 km height. The model time step was dynamically calculated following the CFL stability criterion, not exceeding 5 s. The microphysics is resolved using time splitting (1/3 of dynamic time step). The upper boundary condition is defined as a Rayleigh friction layer with 60 s timescale. The heating rate increases linearly in time from 0 to its prescribed value at time equal to 300 s. To convert the heat flux to convective energy, the McCarter and Broido (1965) factor (0.55) is also used as for the ATHAM runs. The environmental condition for air pressure, temperature, water vapor mixing ratio, horizontal velocity and density were provided by the two rawinsondes described in Sect. 3.1. Fires of 10 and 50 ha were used for the model simulations. Typically, steady state is reached within 50 min, this number being the upper limit of the time integration. The final rise of the plume is determined by the height for which the vertical velocity of the in-cloud air parcel is less than  $1 \text{ m s}^{-1}$ .

### 3.4 Comparison of the 1-D PRM and ATHAM simulations

Figure 4a and b show the 1-D PRM model steady state solutions in the dry and wet ambient cases, respectively. We supposed identical fires burning tropical forest areas with a heat flux of  $80 \text{ kW m}^{-2}$  and a size of 10 ha. The vertical velocity ( $W$ ,  $\text{m s}^{-1}$ ) and vertical mass distribution (VMD, %, see Appendix B for the definition) profiles are

## Smoke plume rise in a windy environment

S. R. Freitas et al.

Title Page

Abstract

Introduction

Conclusions

References

Tables

Figures

◀

▶

◀

▶

Back

Close

Full Screen / Esc

Printer-friendly Version

Interactive Discussion



shown.

For both cases, we also performed a set of runs considering a no-wind hypothesis by setting  $u_e(z)=0$ . We introduced the VMD quantity (as described in Appendix B) to provide the mass detrainment layer for the 1-D simulations and define the vertical emission source field of vegetation fires products of regional or global 3-D atmospheric transport models. The vertical detrainment mass layer is of course not simulated in 1-D models as it is in 2-D or 3-D cloud resolving models such as ATHAM. The VMD definition was based on ATHAM simulated features and provides a probability mass distribution as a function of the vertical velocity profile simulated by the 1-D PRM. For the dry case, panel (A) of Fig. 4, 1-D PRM predicts a cloud top near 4 and 5 km including or not the ambient wind effect, respectively. Thus, in this case, the enhanced entrainment reduced the cloud top by around 1 km. The cloud top predicted by ATHAM (Fig. 3a) was  $\sim 4.8$  km with the aerosol mass detrainment layer localized approximately between 3 and 4.5 km (showed at Fig. 4 as grey filled rectangles). The vertical mass distribution without the ambient wind entrainment coincides well with the ATHAM results, being somewhat broader. The 1-D PRM model, with dynamic entrainment caused by the relative motion between the smoke plume and the ambient air, predicts a lower layer, with approximately the upper half inside the ATHAM detrainment mass zone and the lower half below that. Figure 4c shows the total condensate water (CW), buoyancy acceleration ( $B_a$ ) and entrainment acceleration ( $E_a$ ) for the cases discussed before. With no dynamic entrainment in the model formulation, the plume is capped by a cumulus with a total condensate water of  $\sim 2 \text{ g kg}^{-1}$  near 5 km height. Dynamic entrainment strongly reduces the cumulus properties, not only in terms of the total condensed water (maximum  $\sim 1 \text{ g kg}^{-1}$ ) but also cloud volume. In the forcing terms of vertical equation of motion (Eq. 1), there is a reduction of buoyancy due to enhanced entrainment of drier air. On the other hand, the entrainment deceleration ( $E_a$ ) is increased in the lower levels, due to additional dynamic entrainment. At upper levels,  $E_a$  decreases because  $\delta_{\text{entr}}$  is smaller (since  $u$  is approximately  $u_e$ ) and at the same time the lateral entrainment is smaller due the larger horizontal size of the plume.

## Smoke plume rise in a windy environment

S. R. Freitas et al.

Title Page

Abstract

Introduction

Conclusions

References

Tables

Figures

◀

▶

◀

▶

Back

Close

Full Screen / Esc

Printer-friendly Version

Interactive Discussion



**Smoke plume rise in a windy environment**

S. R. Freitas et al.

[Title Page](#)[Abstract](#)[Introduction](#)[Conclusions](#)[References](#)[Tables](#)[Figures](#)[◀](#)[▶](#)[◀](#)[▶](#)[Back](#)[Close](#)[Full Screen / Esc](#)[Printer-friendly Version](#)[Interactive Discussion](#)

The wet and windy ambient air case is discussed as follows. Profiles of vertical velocity and vertical mass distribution (VMD) are shown in Fig. 4. Inclusion or exclusion of dynamic entrainment results in huge differences. The cloud top predicted by ATHAM (Fig. 3b) was  $\sim 2.5$  km with the aerosol mass detrainment layer localized approximately between 1 and 2.3 km. Without the dynamic entrainment, the predicted 1-D PRM cloud top and mass detrainment layer totally disagree with the corresponding ATHAM simulation. The predicted cloud top is at  $\sim 5.8$  km with a VMD between 2.8 and 5.8 km, far from ATHAM results. With the dynamic entrainment process, 1-D PRM predicts a much lower cloud top around  $\sim 2.6$  km with the mass detrainment layer between 1 and 2.5 km, and now the agreement with ATHAM is significantly improved. For this case, the condensed water and accelerations are shown in Fig. 4d. Because the ambient air is moister in the wet case, not including the dynamic entrainment, the plume is capped by a bigger cumulus with the CW of  $\sim 4$  g kg $^{-1}$  at 5.5 km height. However, because of stronger deceleration caused by the windy environment, the plume stops below the condensation level. No clouds are formed at top of the plume (CW  $\sim 0$ ) and, consequently, there is no additional buoyancy gained from latent heat release. Both processes explain the much lower “cloud” top and injection layer presented in the wet case.

Figure 4f and i introduce the results for bigger fires with size of 50 ha. All other settings remain the same as in the previous cases. The larger size of the fire promotes stronger updrafts and higher clouds tops, similar to ATHAM results. The dry case vertical velocity and mass distribution profiles are shown in panel (f). The difference in the cloud top height caused by dynamic entrainment is about 1 km (from 7 to 6 km). The cloud top predicted by ATHAM (Fig. 3c) was  $\sim 6$  km with the aerosol mass detrainment layer localized approximately between 3 and 5.8 km. The results of the 1-D PRM with the dynamic entrainment present a better agreement with ATHAM simulation in terms of the predicted cloud top as well as the injection layer height and depth, as described by the VMD quantity.

Figure 4g shows the results for the wet and windy ambient air case. As in the case

## Smoke plume rise in a windy environment

S. R. Freitas et al.

Title Page

Abstract

Introduction

Conclusions

References

Tables

Figures

◀

▶

◀

▶

Back

Close

Full Screen / Esc

Printer-friendly Version

Interactive Discussion



of the 10 ha fire, including dynamic entrainment causes much larger changes in the simulated plume rise; the cloud top drops from 8.5 to 5.8 km. The vertical mass distribution not including the dynamic entrainment is centered at 6.5 km extending from 4 to 8.5 km. Due to the enhanced horizontal entrainment associated with relative motion between ambient and plume, the vertical mass distribution center drops to 4.2 km extending from 2.8 to 5.8 km. From ATHAM simulation (Fig. 3d), the predicted cloud top of this case is around 4.9 km with the main detrainment aerosol layer localized between ~2.9 and 4.9 km. Therefore, including the dynamic entrainment results in a much better agreement with ATHAM simulated features, similar to the dry case. 1-D PRM results and discussion of the simulated  $CW$ ,  $B_a$  and  $E_a$  for the 50 ha fire are very similar to the presented for the 10 ha fire size and are shown at panels (h) and (i). However, in this case the smoke plume is capped by a cumulus (panel i), unlike the dry case (panel d), indicating that the smoke plume reached the condensation level due to the stronger initial updraft caused by the larger fire size and the smaller entrainment rates.

## 4 Conclusions

We have extended the 1-D cloud model described in F2007 to include the effect of the ambient wind on the smoke plume rise development associated with vegetation fires. This process is represented by an additional entrainment term proportional to the difference between horizontal wind speeds of the center of mass of the plume and the ambient air. We have shown that this effect has an important impact on the definition of the cloud top and detrainment mass layer mainly for smaller fires under moist and windy situations. To verify the reliability of the physical representation of 1-D model, its results are compared with ones produced using the complex non-hydrostatic 3-D ATHAM model. Our findings suggest that the extended 1-D model can generate feasible simulations when compared to the 3-D model.

The new formulation, when embedded in the 3-D regional or global transport models to determine the vertical mass detrainment layer of smoke associated to vegetation

fires, should improve the simulation of vertical distribution, transport and dispersion of aerosols and trace gases, mainly in areas dominated by small fires, as in savannas, pasture or cropland areas, and/or in a windy environments where the dynamic entrainment processes dominate the cloud-environment horizontal mixing.

5 The new information needed by the extended formulation is the horizontal ambient wind, which is routinely simulated by the large scale 3-D host models. Therefore this new feature is easily implemented and the impact of wind-generated dynamic entrainment process on regional and global smoke distribution predicted. In addition, the vertical mass distribution provides a way that 1-D cloud models can simulate not only  
10 the cloud top but also the actual mass detrainment layers. These are the fundamental quantities needed to determine the emission source field to be used in the 3-D host large scale transport models.

## Appendix A

### 15 The dynamic entrainment formulation

Consider a cylindrical volume of radius  $R$  and depth  $\Delta z$  (see Fig. A1). The in-cloud horizontal mass flux ( $f_h$ ) is given by

$$f_h = \rho_{\text{env}}(u_e - u) \quad (\text{A1})$$

where  $\rho_{\text{env}}$  is the ambient air density and  $u_e$  and  $u$  were defined above. Therefore, the  
20 mass gained by this cloud layer during the time  $\Delta t$  is

$$\Delta m = f_h(2R\Delta z)\Delta t = \rho_{\text{env}}(u_e - u)(2R\Delta z)\Delta t \quad (\text{A2})$$

The definition of the mass entrainment rate is

$$\delta_{\text{entr}} = \frac{1}{m} \frac{\Delta m}{\Delta t}$$

## Smoke plume rise in a windy environment

S. R. Freitas et al.

Title Page

Abstract

Introduction

Conclusions

References

Tables

Figures

◀

▶

◀

▶

Back

Close

Full Screen / Esc

Printer-friendly Version

Interactive Discussion



$$= \frac{1}{\pi R^2 \Delta z \rho_{\text{cloud}}} \frac{\rho_{\text{env}}(u_e - u)(2R \Delta z) \Delta t}{\Delta t} \quad (\text{A3})$$

where  $\rho_{\text{cloud}}$  is the in-cloud air density. Assuming that

$$\rho_{\text{cloud}} \approx \rho_{\text{env}}, \quad (\text{A4})$$

we finish with the following expression for the dynamic entrainment

$$\delta_{\text{entr}} = \frac{2}{\pi R} (u_e - u). \quad (\text{A5})$$

## Appendix B

### The vertical mass distribution (VMD) definition

The definition is based on the well established premise that the main detrainment mass layer of cumulus convection is situated close to the cloud top. ATHAM model results for the vertical velocity profiles (not shown) demonstrated that the main smoke injection layer, defined in terms of the horizontally averaged mass distribution (see Fig. 3), is indeed situated in the upper half part of the cumulus. The upper part is defined beginning at the vertical level where the in-cloud vertical velocity starts to decrease ( $z_i$ ) until the level where it vanishes ( $z_f$ ). Based on this definition, the vertical mass distribution is defined as follows:

- (a) from the 1-D PRM steady state vertical velocity profile, the upper half part of the cumulus is determined in terms of the heights  $z_i$  and  $z_f$  ( $z_f > z_i$ );
- (b) a parabolic function of the height  $z$  with roots at  $z_i$  and  $z_f$  is defined;
- (c) the function is then normalized to 1 in the interval  $[z_i, z_f]$ .

*Acknowledgements.* We acknowledge partial support of this work by CNPq (302696/2008-3, 309922/2007-0) and by the Max Planck Society (MPG). J. T. thanks Stephan Eto for conducting the ATHAM model simulations.

Title Page

Abstract

Introduction

Conclusions

References

Tables

Figures

◀

▶

◀

▶

Back

Close

Full Screen / Esc

Printer-friendly Version

Interactive Discussion



## References

- Bursik, M.: Effect of wind on the rise height of volcanic plumes, *Geophys. Res. Lett.*, 28(18), 3621–3624, 2001. 14715
- Freitas, S. R., Longo, K. M., Chatfield, R., Latham, D., Silva Dias, M. A. F., Andreae, M. O., Prins, E., Santos, J. C., Gielow, R., and Carvalho Jr., J. A.: Including the sub-grid scale plume rise of vegetation fires in low resolution atmospheric transport models, *Atmos. Chem. Phys.*, 7, 3385–3398, 2007, <http://www.atmos-chem-phys.net/7/3385/2007/>. 14714, 14716
- Graf, H.-F., Herzog, M., Oberhuber, J. M., and Textor, C.: The effect of environmental conditions on volcanic plume rise, *J. Geophys. Res.*, 104(D20), 24309–24320, 1999. 14715, 14720
- Herzog, M., Oberhuber, J. M., and Graf, H.-F.: A Prognostic Turbulence Scheme for the Non-hydrostatic Plume Model ATHAM, *J. Atmos. Sci.*, 60, 2783–2796, 2003. 14720
- Latham, D.: A one-dimensional plume predictor and cloud model for fire and smoke managers, General Technical Report INT-GTR-314, Intermountain Research Station, USDA Forest Service, Nov, 1994. 14716, 14719
- Luderer, G., Trentmann, J., Winterrath, T., Textor, C., Herzog, M., Graf, H. F., and Andreae, M. O.: Modeling of biomass smoke injection into the lower stratosphere by a large forest fire (Part II): sensitivity studies, *Atmos. Chem. Phys.*, 6, 5261–5277, 2006, <http://www.atmos-chem-phys.net/6/5261/2006/>. 14720
- McCarter, R. and Broido, A.: Radiative and convective energy from wood crib fires, *Pyrokinetics*, 2, 65–85, 1965. 14721
- Oberhuber, J. M., Herzog, M., Graf, H.-F., and Schwanke, K.: Volcanic plume simulation on large scales, *J. Volcanol. Geotherm. Res.*, 87, 29–53, 1998. 14720
- Textor, C., Graf, H.-F., Herzog, M., and Oberhuber, J. M.: Injection of gases into the stratosphere by explosive volcanic eruptions, *J. Geophys. Res.*, 108(D19), 4606, doi:10.1029/2002JD002987, 2003. 14720
- Textor, C., Graf, H. F., Herzog, M., Oberhuber, J. M., Rose, W. I., and Ernst, G. G. J.: Volcanic particle aggregation in explosive eruption columns. Part I: Parameterization of the microphysics of hydrometeors and ash, *J. Volcanol. Geotherm. Res.*, 150, 359–377, 2006. 14720
- Trentmann J., Andreae, M. O., Graf, H.-F., Hobbs, P. V., Ottmar, R. D., and Trautmann, T.: Simulation of a biomass-burning plume: Comparison of model results with observations, *J. Geophys. Res.*, 107(D2), 4013, doi:10.1029/2001JD000410, 2002. 14720

## Smoke plume rise in a windy environment

S. R. Freitas et al.

Title Page

Abstract

Introduction

Conclusions

References

Tables

Figures

◀

▶

◀

▶

Back

Close

Full Screen / Esc

Printer-friendly Version

Interactive Discussion



Trentmann, J., Luderer, G., Winterrath, T., Fromm, M. D., Servranckx, R., Textor, C., Herzog, M., Graf, H.-F., and Andreae, M. O.: Modeling of biomass smoke injection into the lower stratosphere by a large forest fire (Part I): reference simulation, *Atmos. Chem. Phys.*, 6, 5247–5260, 2006,

5 <http://www.atmos-chem-phys.net/6/5247/2006/>. 14720

Turner, J. S.: *Buoyancy effects in fluids*, Cambridge Univ. Press, Cambridge, 368 pp., 1973. 14719

ACPD

9, 14713–14733, 2009

---

## Smoke plume rise in a windy environment

S. R. Freitas et al.

---

Title Page

Abstract

Introduction

Conclusions

References

Tables

Figures

◀

▶

◀

▶

Back

Close

Full Screen / Esc

Printer-friendly Version

Interactive Discussion



**Smoke plume rise in a windy environment**

S. R. Freitas et al.



**Fig. 1.** Photographs of the smoke plume rise produced from two deforestation fires in the Amazon basin under calm (left) and windy (right) environments. Both photos were taken from aircraft. Note that size of the fires and the plume height differs substantially between the plumes. (Pictures taken by M. O. Andreae and M. Welling.)

[Title Page](#)[Abstract](#)[Introduction](#)[Conclusions](#)[References](#)[Tables](#)[Figures](#)[I◀](#)[▶I](#)[◀](#)[▶](#)[Back](#)[Close](#)[Full Screen / Esc](#)[Printer-friendly Version](#)[Interactive Discussion](#)

## Smoke plume rise in a windy environment

S. R. Freitas et al.

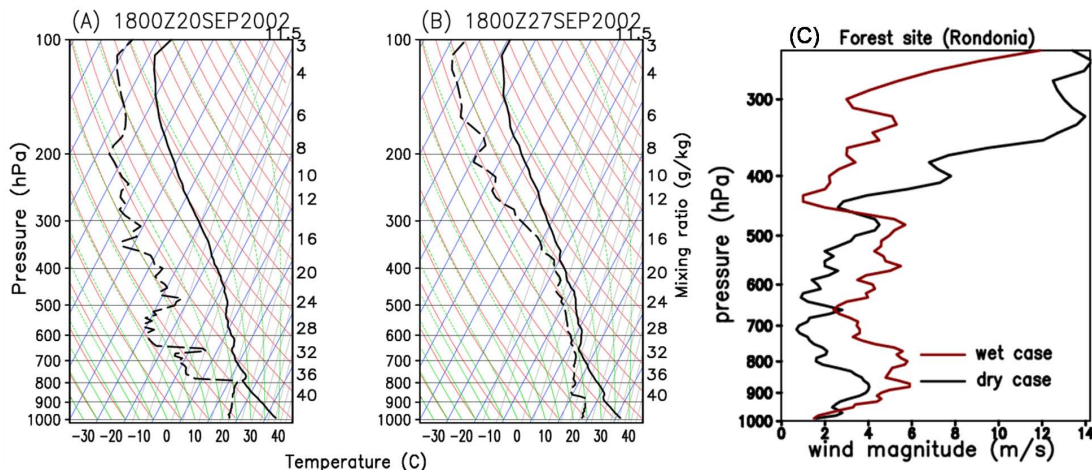


**Fig. 2.** Temperature (solid) and dew point temperature (dashed) profiles from a rawinsonde launched in Rondonia (11 S, 60 W) shown by a skew  $T$ -log  $p$  diagram. Case **(A)** depicts the condition at 1800Z on 20 September 2002, classified as the dry case. **(B)** is the wet case corresponding to 1800Z on 27 September 2002 (reproduced from Freitas et al., 2007). **(C)** Horizontal wind magnitude profiles of the dry (black) and wet (red) cases obtained from the rawinsondes.

[Title Page](#)[Abstract](#)[Introduction](#)[Conclusions](#)[References](#)[Tables](#)[Figures](#)[I◀](#)[▶I](#)[◀](#)[▶](#)[Back](#)[Close](#)[Full Screen / Esc](#)[Printer-friendly Version](#)[Interactive Discussion](#)

Smoke plume rise in  
a windy environment

S. R. Freitas et al.

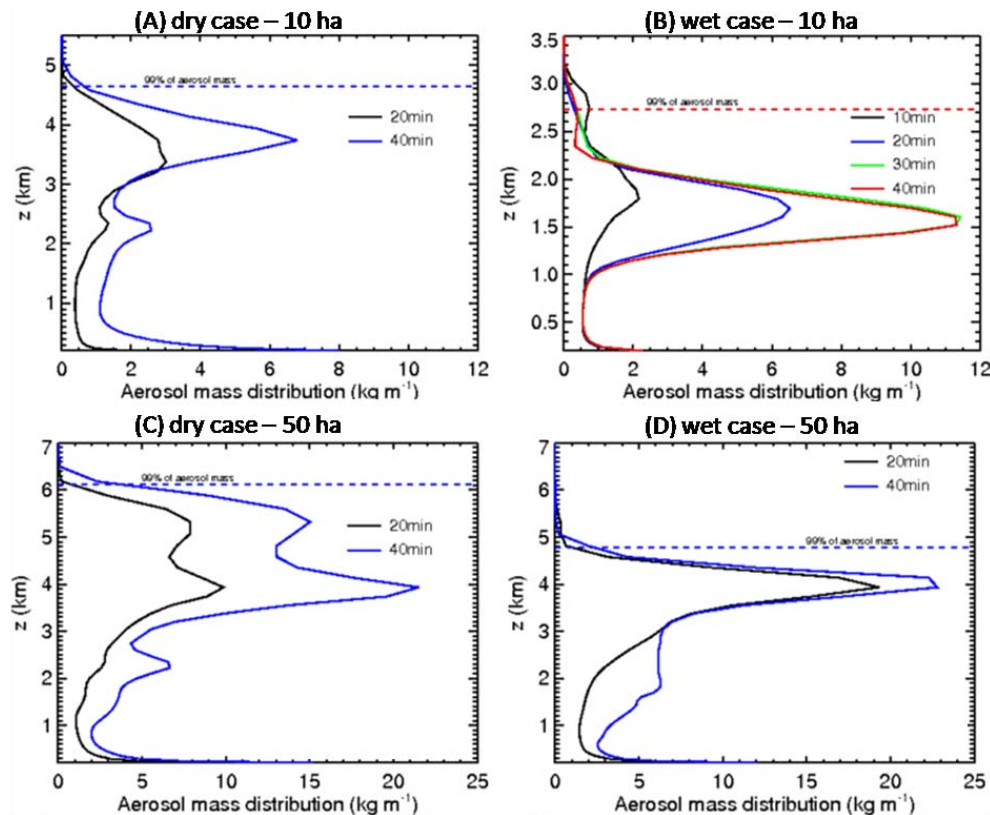


**Fig. 3.** Horizontally averaged aerosol mass distribution ( $\text{kg m}^{-3}$ ) as simulated by the ATHAM model for the dry (A, C) and wet (B, D) cases. Model results for a fire with size of 10 ha (A, B) and 50 ha (C, D). All simulations used a heat flux of  $80 \text{ kW m}^{-2}$ .

[Title Page](#)[Abstract](#)[Introduction](#)[Conclusions](#)[References](#)[Tables](#)[Figures](#)[I◀](#)[▶I](#)[◀](#)[▶](#)[Back](#)[Close](#)[Full Screen / Esc](#)[Printer-friendly Version](#)[Interactive Discussion](#)

## Smoke plume rise in a windy environment

S. R. Freitas et al.

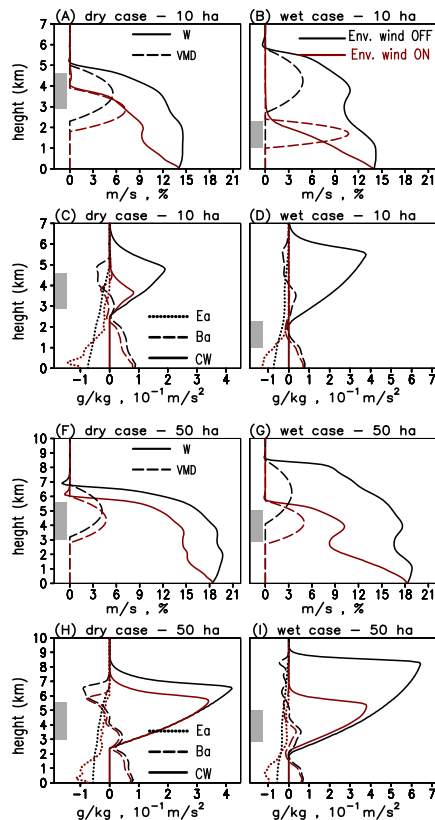


**Fig. 4.** Plume model steady state solution for the dry (fire size of 10 ha: **(A)** and **(C)**; 50 ha: **(F)** and **(H)**) and wet (fire size of 10 ha: **(B)** and **(D)**; 50 ha: **(G)** and **(I)**) and heat flux of  $80 \text{ kW m}^{-2}$ . The quantities are: vertical velocity ( $W$ ,  $\text{m s}^{-1}$ ), vertical mass distribution (VMD, %), entrainment acceleration ( $E_a$ ,  $10^{-1} \text{ m s}^{-2}$ ), buoyancy acceleration ( $B_a$ ,  $10^{-1} \text{ m s}^{-2}$ ), and total condensate water (CW,  $\text{g kg}^{-1}$ ). Model results considering the actual ambient wind are in red and the ambient at rest in black colors. The grey rectangles indicate the main injection layer simulated by the ATHAM model.

Title Page

Abstract

Introduction

Conclusions

References

Tables

Figures

◀

▶

◀

▶

Back

Close

Full Screen / Esc

Printer-friendly Version

Interactive Discussion



**Smoke plume rise in a windy environment**

S. R. Freitas et al.

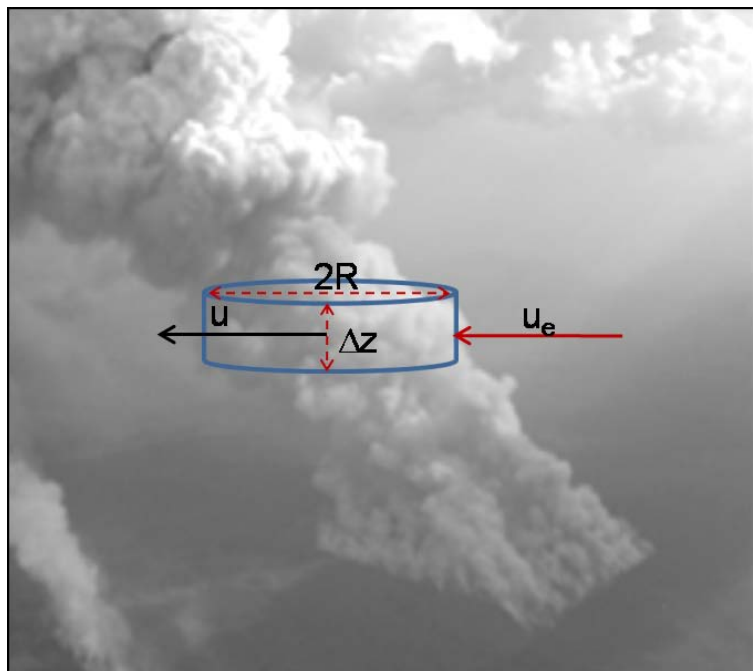


**Fig. A1.** The description of the dynamic entrainment rate formulation (picture taken by M. Welling).

[Title Page](#)[Abstract](#)[Introduction](#)[Conclusions](#)[References](#)[Tables](#)[Figures](#)[I◀](#)[▶I](#)[◀](#)[▶](#)[Back](#)[Close](#)[Full Screen / Esc](#)[Printer-friendly Version](#)[Interactive Discussion](#)